Resistance surface concept for concrete fracture

V. Veselý & Z. Keršner
Institute of Structural Mechanics, Civil Engineering Faculty, Brno University of Technology, Brno, Czech Republic

ABSTRACT: Resistance surface concept is presented in the paper, which brings a new perspective into the part of fracture mechanics of quasi-brittle materials. This concept is based on equivalent elastic crack models and resistance curves (*R*-curves) with the extension to the three-dimensional space. Third dimension is constraint parameter *T*-stress or dimensionless biaxiality factor *B* evaluated at the elastic equivalent crack tip. It results from experimental and numerical studies, that *R*-curves of specimens with various testing configurations possibly are subsets of a *R*-surface. In the paper four typical testing configurations with different constraint conditions are studied: three point bending of notched beam, double edge notched cube under eccentric compression, double edge notched cube under uniaxial tension and single edge notched cube under compact tension.

Keywords: equivalent elastic crack, *R*-curve, stress multiaxiality, *T*-stress, biaxiality factor, *R*-surface

1 INTRODUCTION

1.1 *Equivalent elastic crack models and R-curves*

Although the class of equivalent elastic crack models and following *R*-curve concept is only the lowest order non-linear approximation of true concrete cracking behavior and more complex and general models have been recently proposed, it has still a great potential in some cases to be used as an effective tool for concrete behavior modeling and structural analysis. The main reason is the relatively easy handling formalism of linear elastic fracture mechanics (LEFM), which is employed by the models of equivalent elastic crack. For certain types of analyses equivalent elastic crack models and *R*-curves could be more than suitable and can save much analyst's effort in comparison to time-, computationally- and/or economically-demanding analyses using cohesive crack, crack band, non-local, particle models etc.

Different equivalent elastic crack models were proposed in the last 30 years: starting from Irwin's application to metals, following by Jenq-Shah (Jenq & Shah 1985) and Nallathambi-Karihaloo (Nallathambi & Karihaloo 1986) models for concrete and culminating by Bažant's size effect model (Bažant 1984), which merges previous concrete elastic equivalent crack models for large sizes. However, all equivalent elastic crack models and related *R*-curves have a crucial disadvantage: they are not independent of the specimen geometry and testing setup. Aside from the asymptotic Bažant's size effect model dealing with specimens of infinite dimensions, from which the geometry independence of its parameters arises, and aside from the method of *R*-curve determination from Bažant's size effect law (Bažant & Kazemi 1990).

1.2 *Capturing of geometry effect by parameters of constraint*

Load (even uniaxial) applied to a pre-cracked specimen is decomposed at the discontinuity tip causing a triaxial state of stress in the region. So created stress multiaxiality is affected by the structural shape and loading configuration. Different constraint of deformation near the crack tip caused by different stress multiaxiality (due to different geometry and testing conditions) leads into non-universality of determined fracture parameters, in particular K_{Ic} (Knésl & Bednář 1998, Knésl et al. 2000).

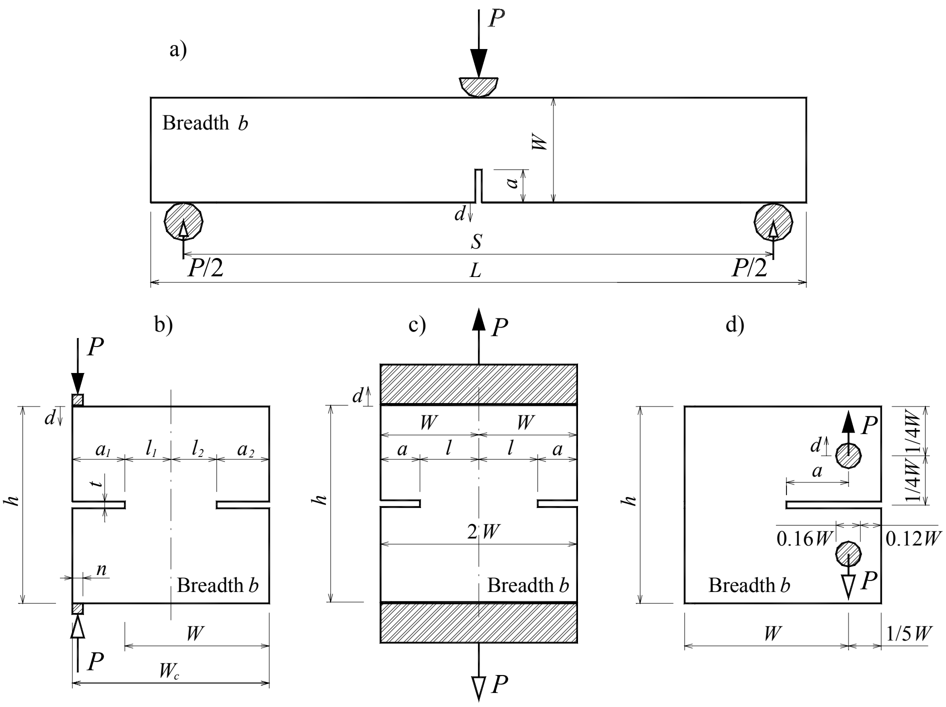

Figure 1. Testing configurations studied: a) SEN-TPB, b) DEN-EC, c) DEN-T and d) SEN-CT

The problem of dependence of these parameters on the specimen shape and test configuration (the constraint effect) is captured successfully by more detailed description of stress field near the crack tip in the elastic and elasto-plastic fracture mechanics of metals. This approach is called two-parametric fracture mechanics. It is based on two members of Williams's series approximating the crack tip stress field that are taking into account instead of one in the classical fracture mechanics approach.

In two-parametric LEFM the first member of Williams's series is related to K-factor with $r^{-1/2}$ singularity (r is the radial distance from the crack tip), whereas the second member corresponds to T-stress independent of r. Values of T-stress or equivalent biaxiality factor B (dimensionless) can serve as a measure of constraint effect.

1.3 *Resistance surface concept*

This paper proposes a synthesis of equivalent elastic crack models and related R-curves with two-parametric LEFM. The dependence of crack growth resistance R (equivalently K_R) on equivalent elastic crack extension Δa is known as the resistance curve (R-curve, equivalently K_R-curve) form which complete quasi-brittle concrete behavior can be predicted. But disadvantage is the shape dependence mentioned above. However, geometry dependent R-curves for different testing configurations characterized by various constraint conditions at the equivalent elastic crack tip are possible to draw to a three dimensional plot. The third dimension is a constraint parameter B (or T).

From experimental and numerical studies carried out at Brno University of Technology it seems that R-curves of specimens with various constraint conditions (testing configuration) are subsets of a R-surface which can be considered as a material parameter. If this hypothesis is valid, then for prediction of fracture behavior of any specimen or structure one could use a R-curve that is derived as a section of the characteristic R-surface after this manner: the R-surface is cut by a ruled surface given by a course of constraint characteristics B (or T) related to investigated case. The intersection of those two surfaces can be treated as a R-curve appropriate to the specimen geometry and testing setup. Then complete fracture analysis can be carried out.

2 NUMERICAL EXPERIMENT

Proposed approach was introduced by Veselý & Keršner 2003 through the numerical study on four testing configurations (see Figure 1) with different constraint conditions (see Figure 2). Three point bending of notched beam (SEN-TPB), double edge notched cube under eccentric compression (DEN-EC), double edge notched cube under uniaxial tension (DEN-T) and single edge notched cube under compact tension (SEN-CT), each with four relative notch lengths, were "numerically" tested and load-displacement (*P–d*) diagrams were recorded. Loading curves were gained by means of non-linear FEM simulations (commercial FEM code based on crack band model – Červenka & Pukl 2003) after its calibration according to experimental results on SEN-TPB and DEN-EC specimens (*P–d* diagrams of all geometries could not be gained experimentally because of insufficiently equipped laboratory).

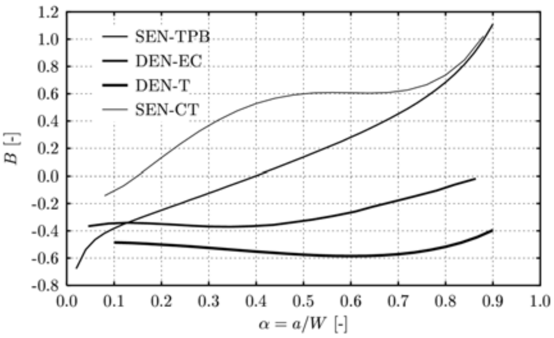

Figure 2. Biaxiality factor B as a function of relative crack length for analyzed geometries

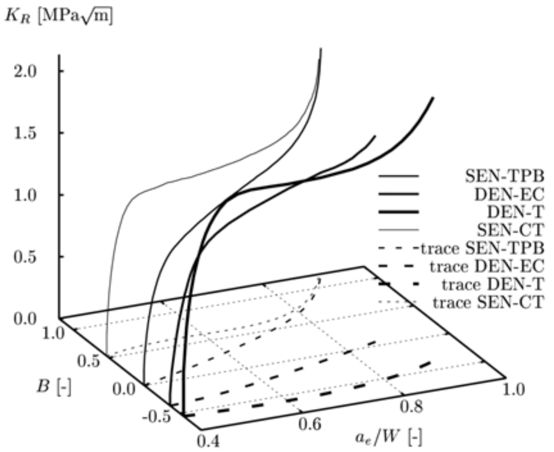

Figure 3. K_R-curves from compliance for testing configurations with different constraint of deformation near the elastic equivalent crack tip drawn into 3D plot

K_R-curves based on unloading compliance measurements of equivalent elastic crack extension were computed from simulated *P–d* diagrams. By K_R-curves the dependence of effective fracture toughness (according to Nallathambi-Karihaloo model) on the equivalent elastic crack length is meant (not the crack extension resistance computed from cohesive stress by the Xu-Reinhardt approach – Xu & Reinhardt 1998, Reinhardt & Xu 1999). The functions of constraint characteristic B as a dependence of the relative crack length a/W were gained by elastic FEM analysis of near tip crack field for all geometries. Finally, resistance surfaces (in space K_R–(a_e/W)–B) were constructed from compliance technique determined K_R-curves corresponding to mentioned testing geometries for several initial notch lengths. One of calculated K_R-surfaces is sketched in Figure 3.

In this paper the approach is tested through R-surfaces gained from R-curves determined in a different way; R-surface for a testing geometry is here defined as a union of R-curves for all initial notch lengths of analyzed specimen from Bažant's size effect law. The same four testing configurations from Figure 1 were taken into consideration (Veselý & Keršner 2003).

2.1 *R-curves from size effect law*

The analytical determination of the R-curve from size effect law was developed by Bažant & Kazemi 1990 and provides the shape of R–Δa curve in explicit parametric form by means of coordinates $\Delta a/c_f$ and R/G_f, where c_f and G_f are parameters of Bažant's size effect law:

$$\frac{\Delta a}{c_f} = f_1(\alpha') = \left[\frac{k(\alpha')}{2k'(\alpha')} - (\alpha' - \alpha_0)\right]\frac{2k'(\alpha_0)}{k(\alpha_0)} \qquad (1)$$

$$\frac{R}{G_f} = f_2(\alpha') = \frac{k(\alpha')\,k'(\alpha')}{k(\alpha_0)\,k'(\alpha_0)} f_1(\alpha') \qquad (2)$$

Both coordinates are functions of geometry factor $k(\alpha)$ and its derivative $k'(\alpha)$. The parameter α' of the expressions is defined as the value $\alpha = a/D$ for which a specimen of size D reaches the peak load (Bažant & Planas 1998); α_0 is relative length of initial crack. To draw R–Δa curve for particular material and loading configuration a set of suitable values of parameter α' must be chosen and then functions $f_1(\alpha')$ and $f_2(\alpha')$ are evaluated. Then coordinates [Δa, R] of points of the R-curve are calculated from size effect law parameters c_f and G_f, which are constants for given material.

2.2 *T-stress and biaxiality factor B*

The characterization of stress, strain, and displacement fields at the tip of a crack is fundamental to fracture mechanics. We focus on opening mode of loading (mode I) in next steps. Stress-strain field is described by bi-harmonic equation of equilibrium in case of elastic body:

$$\Delta\Delta\,\Phi = 0 \tag{3}$$

where Δ is double Laplace's operator and Φ is Airy's function. The solution is being found in the shape of infinite series:

$$\Phi = \sum_{k=1}^{\infty} a_k\, r^{\lambda_k} f_k\left(\lambda_k, \theta\right) \tag{4}$$

where r, θ are polar coordinates, λ_k is eigenvalue, and f_k eigen function. Tensor of stresses can be expressed in the form of Williams's series from this solution (Knésl & Bednář 1998):

$$\sigma_{ij} = \sum_{n=1}^{\infty} \left(A_n \frac{n}{2} \right) r^{\frac{n}{2}-1} f_{ij}\left(n, \theta\right) \tag{5}$$

Two-parameter fracture mechanics takes into account first two members of this series; the stress tensor can be then written as

$$\sigma_{ij} = \frac{K_I}{\sqrt{2\pi r}} f_{ij}\left(\theta\right) + T\,\delta_{1i}\delta_{1j} \tag{6}$$

where K_I is stress intensity factor, $f_{ij}(\theta)$ known function of polar angle θ, and δ_{kl} is Cronecker delta. The first parameter is typically used to quantify the amplitude of the stress field, the second parameter is used to index the effects of constraint at the crack tip – the T-stress is a measure of the in-plane constraint in an elastic body. The constraint effect can be equivalently characterized by a dimensionless factor of stress biaxiality B:

$$B = \frac{T\sqrt{\pi a}}{K_I} \tag{7}$$

where a = length of crack.

There are several methods to determine the constraint characteristics published in the literature. Nowadays, the most frequently used are those

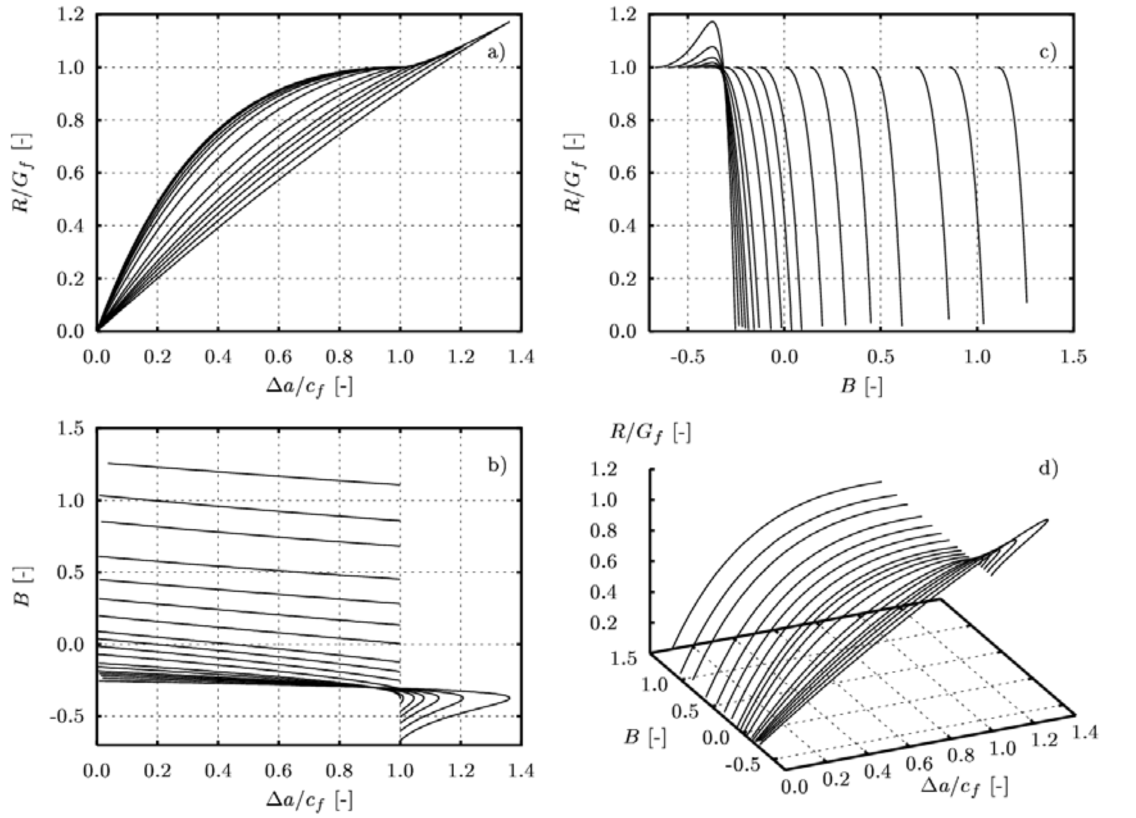

Figure 4. R-surface for SEN-TPB configuration constructed from size effect law R-curves for relative notch lengths 0.02, 0.03, 0.04, 0.05, 0.06, 0.08, 0.1, 0.15, 0.2, 0.25, 0.3, 0.4, 0.5, 0.6, 0.7, 0.8, 0.85 and 0.9 (from bottom to top in graph b)

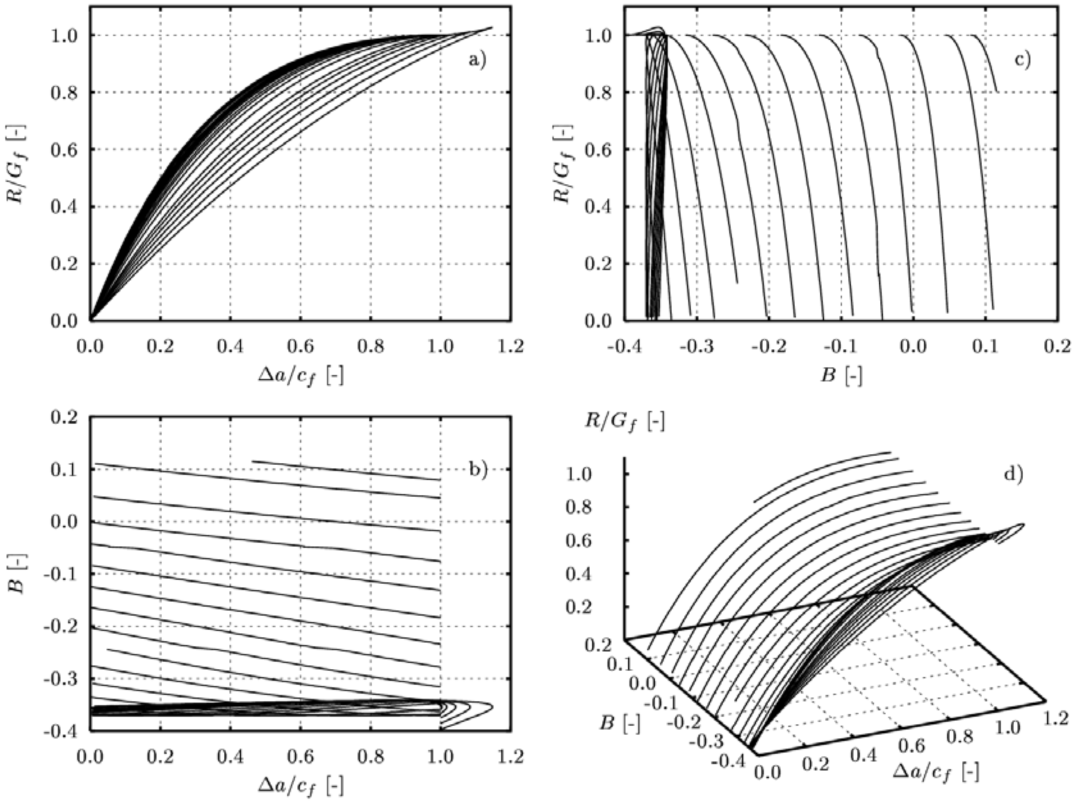

Figure 5. R-surface for DEN-EC configuration from R-curves for relative notch lengths 0.05, 0.06, 0.07, 0.08, 0.09, 0.1, 0.125, 0.15, 0.175, 0.2, 0.25, 0.3, 0.35, 0.4, 0.45, 0.5, 0.55, 0.6, 0.65, 0.7, 0.75, 0.8, 0.85 and 0.875 (from bottom to top in graph b)

based on finite or boundary element analysis (Ayatollahi et al. 1998, Knésl 1995, Gröger 2003). A direct difference technique was employed in this work which matches numerical FEM results to analytical solution.

2.3 *R-surfaces*

In Figures 4, 5, 6 and 7 R-curves for chosen configurations corresponding to relative notch lengths marked in the captions are displayed. They are drawn into space $\Delta a/c_f$, B and R/G_f. It is obvious, that the curves create a surface. Construction of the 3D R-curves for chosen geometry and initial relative crack length α_0 was programmed as follows: the R-curves from Bažant's size effect law were calculated for different initial notch lengths and then a value of biaxiality factor B (function $B(\alpha)$ – see Figure 2) was assigned to each point [$\Delta a/c_f$, R/G_f] of calculated R-curves. It was carried out for each point [$\Delta a/c_f$, R/G_f] appropriate to parameter α' according to the actual $\alpha = a/W$ (= α' if we assume that $W = D$).

3 CONCLUSIONS

3.1 *General remarks*

This paper proposes the resistance surface concept which extends the classical two-dimensional space for displaying of R-curves to three-dimensional one. The third dimension should be a quantity which captures the influence of structural shape and loading conditions on the structural fracture behavior. Parameters of constraint of deformation, such as T-stress or biaxiality factor B, at the elastic equivalent crack tip can be used in this context, although application of tools of two-parameter linear elastic fracture mechanics is not usual in failure models of cementitious composites. It is clear, that its applicability is relevant only as long as the concept of elastic equivalent crack models and R-curves is employed, because both two-parameter LEFM and elastic equivalent models handle with sharp crack.

The resistance surface concept brings a new perspective into the part of quasi-brittle fracture of concrete, mortar, plaster etc. Especially following features of proposed concept are worth noticing:

- The method of Bažant and Kazemi for *R*-curve determination from size effect law provides for certain geometries and initial notch lengths such shapes of R–Δa curve which are ambiguous and inconsistent with the definition of function. On the contrary the plot of such a curve in the proposed extended 3D space immediately gives an explanation. For example *R*-curves of SEN-CT configuration for relative notch lengths shorter than 0.2 are characterized by a specific point, where the R–Δa curve cuts itself making a loop (Figure 7a). From the next graphs in Figure 7 it is obvious that the loop is caused by certain 2D view of curve traversing in 3D space.
- Some *R*-curves drawn in Figures 4, 5 and 7 show interesting behavior just before they reach the plateau (in R/G_f–$\Delta a/c_f$ graph the plateau starts at point with coordinates [1,1]). The part of *R*-curve before reaching the plateau is typically rising, as it is evident from most of *R*-curves in Figures 4, 5, 6 and 7. However, some *R*-curves for SEN-TPB, DEN-EC and SEN-CT configuration (Figures 4, 5 and 7), mainly for very small relative notch lengths (α_0 < 0.15), show different trend. Before they join the beginning of the plateau they achieve considerably higher values than 1 in both coordinates. We note here, that all analyzed geometries are positive ($k'(\alpha_0) > 0$), so the Bažant and Kazemi method to determine *R*-curve from size effect law should work properly in our cases.
- *R*-surface for DEN-T and partly for DEN-EC is folded in the region of lower values of *B*.
- The aforementioned hypothesis of one *R*-surface as the material property was not confirmed. The differences between *R*-surfaces of studied geometries are significant in region of low and negative biaxiality factor. However, for higher positive values of *B* (approximately higher than 0.5) there are immaterial differences between *R*-surfaces of SEN-TPB and SEN-CT (neither DEN-EC nor DEN-T reach the region). To validate hypothesis of

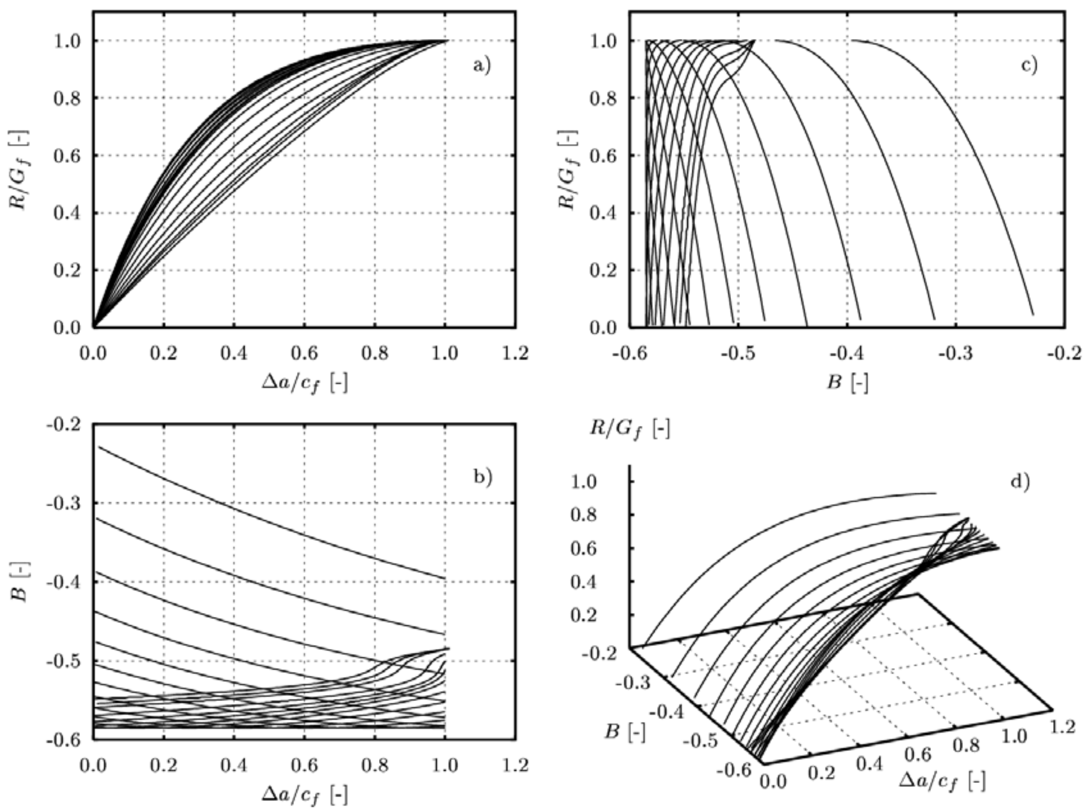

Figure 6. *R*-surface for DEN-T configuration from *R*-curves for relative notch lengths 0.06, 0.08, 0.1, 0.15, 0.2, 0.25, 0.3, 0.35, 0.4, 0.45, 0.5, 0.55, 0.6, 0.65, 0.7, 0.75, 0.8, 0.85 and 0.9 (from bottom to top in graph a)

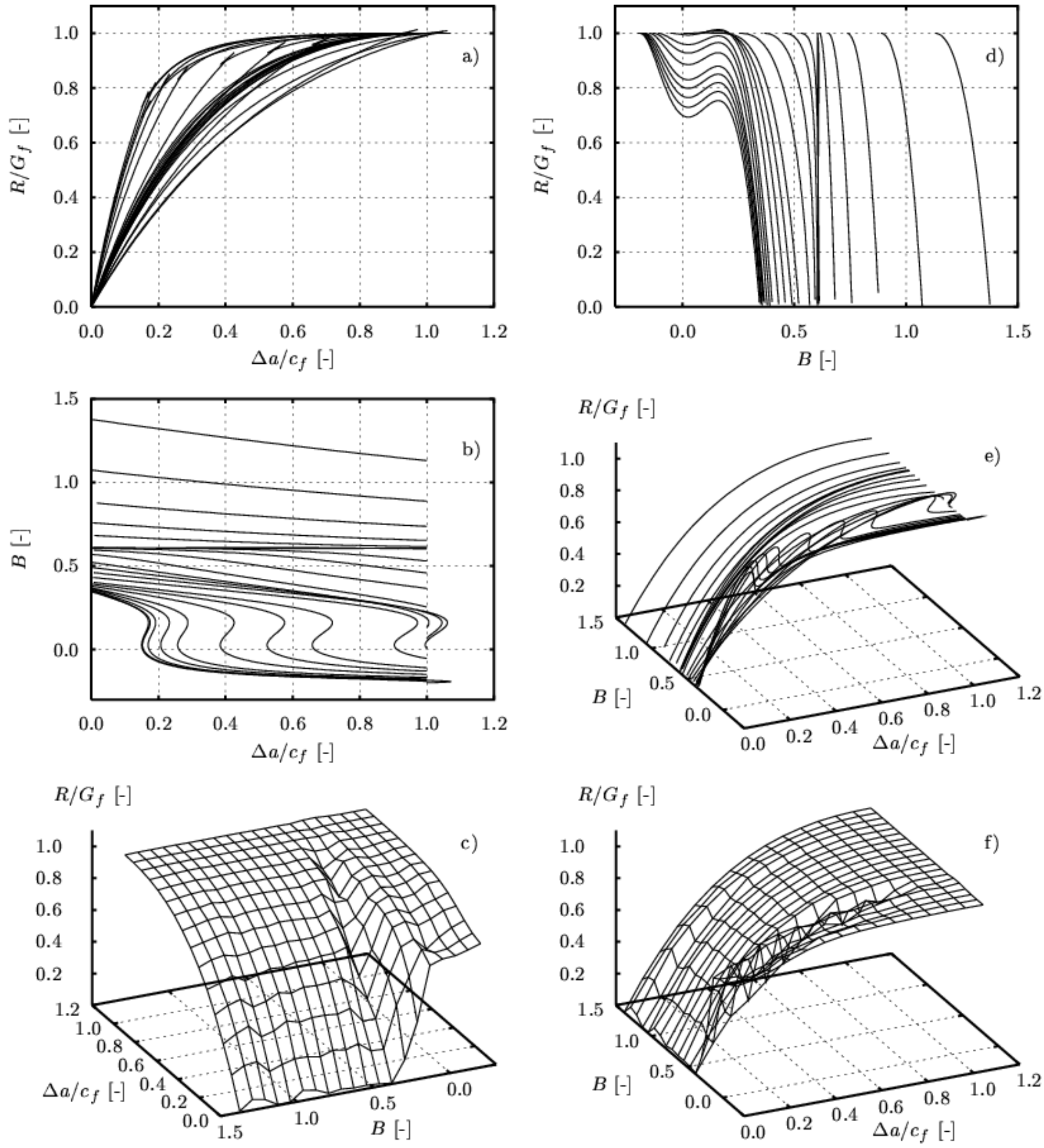

Figure 7. *R*-surface for SEN-CT configuration from *R*-curves for relative notch lengths 0.05, 0.055, 0.06, 0.065, 0.07, 0.08, 0.09, 0.1, 0.125, 0.15, 0.175, 0.2, 0.25, 0.3, 0.35, 0.4, 0.5, 0.6, 0.7, 0.75 0.8, 0.85 and 0.9 (from bottom to top in graph b). An approximation of the surface is sketched in two views in graph c) and f)

possible existence of one *R*-surface which is characteristic for material and independent of geometry other third dimension must be found.

- Interesting and important facts result from resistance surface concept to the structural analysis carried out by means of equivalent elastic crack models and *R*-curves. A quasi-brittle structure with relative notch length α_0 will generally not follow the *R*-curve from size effect constructed for actual structural geometry with actual notch length α_0 during fracture process, but a “true” *R*-curve will rule the crack propagation. This “true” *R*-curve is extracted from *R*-surface for corresponding structural shape, loading, and material as a intersection of *R*-surface and function of *B*. The measure of cogency of true *R*-curve with *R*-curve from size effect depends on structural dimensions. More detailed explanation is introduced in the following example.

3.2 *Experimental example*

We assume notched beam subjected to three point bending. The dimensions of the beam are: width $W = D$ = 80 mm, breadth B = 84 mm, loading span S = 400 mm, length L = 480 mm and notch length a_0 = 26 mm. The beam is made of concrete for which Bažant's size effect law parameters were found: G_f = 45 Jm^{-2}, c_f = 47 mm. In order to make a structural analysis of the beam (i.e. for example to predict the *P–d* diagram) by means of *R*-curve concept one must determine the *R*-curve corresponding to required case. This *R*-curve must depend on material, shape of the structure and loading conditions.

First *R*-surface is determined from *R*-curves from size effect for several relative notch lengths α_0 calculated for SEN-TPB configuration (see Figure 4). This *R*-surface is then transformed using values G_f and c_f to absolute coordinates (see Figure 8). Function $B(\alpha)$ (Figure 2) is also shifted to graph with absolute coordinates transforming it to $B(a)$ using W (see Figure 8). The true *R*-curve which describes the crack propagation of studied notched beam is an intersection of the *R*-surface and function (surface) B. The situation is illustrated in the Figure 8: the *R*-surface is represented by a set of *R*-curves from size effect law and the $B(\alpha)$ function (ruled surface) is cutting the *R*-surface producing the true *R*-curve (drawn in bold, line joining points of intersection of *R*-curves from size effect law and the $B(\alpha)$ function).

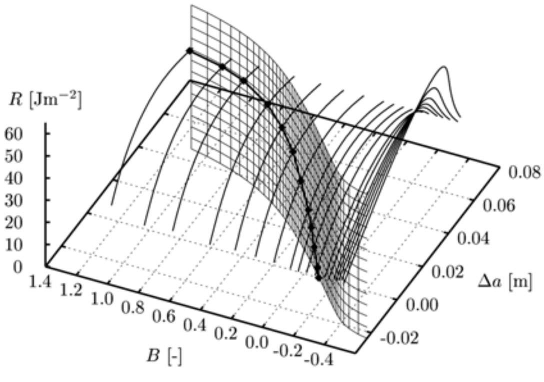

Figure 8. Extraction of "true" *R*-curve corresponding to specific case of geometry and size as an intersection of the *R*-surface with surface characterizing change of constraint of deformation during fracture (function *B*)

In this case the function B traverses the whole *R*-surface before it reaches the plateau. As it is obvious, it depends on the size of the structure how much the *R*-surface is traversed by function B. For larger sizes the true *R*-curve reaches the plateau earlier than fracture process zone is developed through the whole ligament. For infinite size, of course, the true *R*-curve follows the *R*-curve determined from size effect law.

ACKNOWLEDGEMENT

Support for this work was provided by the projects No. 103/03/0006 and No. 103/03/1350 by the Grant Agency of the Czech Republic.

REFERENCES

Ayatollahi, M. R., Pavier, M. J., Smith D. J. 1998 Determination of T-stress from finite element analysis for mode I and mixed mode I/II loading. *International Journal of Fracture* 91: 283-298.

Bažant Z. P. 1984 Size effect in blunt fracture: concrete, rock, metal. *Journal of Engineering Mechanics* 104: 518-535.

Bažant, Z. P. & Kazemi, M. T. 1990 Determination of fracture energy, process zone, length and brittleness number from size effect, with application to rock and concrete. *International Journal of Fracture* 44(2): 111-131.

Bažant, Z. P. & Planas, J. 1998 *Fracture and size effect in concrete and other quasi-brittle materials*. Boca Raton: CRC Press.

Červenka, V. & Pukl, R. 2003 *ATENA Program documentation*. Prague: Červenka Consulting.

Gröger, R. 2003 *Characterization of fracture-mechanical behavior of bimaterial V-notches using BEM*. Ph.D. Thesis. Brno University of Technology, Faculty of Mechanical Engineering, Institute of Solid Mechanics.

Jenq, Y. S. & Shah, S. P. 1985 A two-parameter fracture model for concrete. *ASCE Journal of Engineering Mechanics* 111(10): 1227-1241.

Karihaloo, B. L. 1995 *Fracture mechanics and structural concrete*. New York: Longman Scientific & Technical.

Knésl, Z. 1995 Evaluation of the elastic T-stress using a hybrid finite element approach. *International Journal of Fracture* 70: 9-14.

Knésl, Z. & Bednář, K. 1998 Two-parameter characterization in fracture mechanics. *Engineering Mechanics* 5(3): 133-142.

Knésl, Z., Bednář, K. & Radon, J. 2000 Influence of T-stress on the rate of propagation of fatigue cracks. *Physical Mesomechanics* 3(5): 5-9.

Nallathambi, P. & Karihaloo, B. L. 1986 Determination of specimen-size independent fracture toughness of plain concrete. *Magazine of Concrete Research* 38(135): 67-76.

Reinhardt, H. W. & Xu, S. 1999 Crack extension resistance based on the cohesive force in concrete. *Engineering Fracture Mechanics* 64: 563-587.

Xu, S. & Reinhardt, H. W. 1998 Crack extension resistance and fracture properties of quasi-brittle softening materials like concrete based on the complete process of fracture. *International Journal of Fracture* 92: 71-99.

Veselý, V. & Keršner, Z. 2003 Modified R-curve concept for description of concrete fracture. In Jiří Brožovský (ed.), *Modeling in Mechanics; Proc. workshop, Ostrava, 16 January 2003*. In Czech.